ChemComm

COMMUNICATION

View Article Online
View Journal | View Issue

Cite this: *Chem. Commun.*, 2021, **57**, 10911

Received 10th August 2021,
Accepted 24th September 2021

DOI: 10.1039/d1cc04383h

rsc.li/chemcomm

Zn^{2+}-Dependent peptide nucleic acid-based artificial ribonucleases with unprecedented efficiency and specificity†

Olivia Luige,[a] Partha Pratim Bose,[a] Rouven Stulz,[abc] Peter Steunenberg,‡[a] Omar Brun,§[a] Shalini Andersson,[b] Merita Murtola*[a] and Roger Strömberg *[a]

We present Zn^{2+}-dependent dimethyl-dipyridophenazine PNA conjugates as efficient RNA cleaving artificial enzymes. These PNAzymes display site-specific RNA cleavage with 10 minute half-lives and cleave clinically relevant RNA models.

Modified oligonucleotides (ONs) such as gapmer antisense (ASO) and small interfering RNA (siRNA) technologies are powerful therapeutics used in the treatment of life-threatening diseases.[1,2] Both strategies rely on the recruitment of endogenous enzymes (RNase H or RISC complex, respectively), which results in cleavage of the RNA targets.[1] The complexes of RNA with these ONs must be recognised as substrates for the respective enzymes, which limits the modifications that can be incorporated.[1,3] The chemical design of these ONs is, in turn, linked to issues affecting these technologies such as off-target effects and sequence- and chemistry-dependent toxicity.[3,4] The reliance on cellular enzymes can also lead to non-specific toxicity due to the saturation of endogenous RNA processing pathways.[5]

Oligonucleotide-based artificial (ribo)nucleases (OBANs)[6–8] aim to offer an alternative technology for the reduction of RNA levels, independent of endogenous enzymes. These artificial constructs consist of an ON backbone and a covalently linked "molecular scissors" moiety, which together ensure sequence-specific target recognition followed by catalytic cleavage of the RNA target.[9–11]

Three types of artificial ribonucleases have been investigated in recent years, including Cu^{2+} or Zn^{2+} cofactor dependent PNA–neocuproine conjugates (PNAzymes),[12–15] metal independent tris(2-aminobenzimidazole)-DNA/LNA mixmer conjugates,[16,17] and peptidyl-oligonucleotide conjugates (POCs) that consist of hairpin DNA or 2′-OMe ONs and a catalytic arginine and leucine-rich peptide.[18–20] The metal-free systems, although attractive due to their promise of self-reliance, suffer from low rates of RNA cleavage[16,20] and the aforementioned POCs require assistance from cellular enzymes (RNase H) to achieve turnover of the substrate.[20] Cu^{2+}-Dependent PNAzymes cleave their RNA targets site-specifically with half-lives in the 20–30 minute range and also give turnover.[12,14,15] However, Cu^{2+} PNAzymes are not ideally suited for therapeutic applications, since a sufficient copper ion concentration is required to maintain their activity, while free copper is virtually not available in cells.[21] Zn^{2+} is an attractive cofactor for artificial nucleases due to its presence in various concentrations in intracellular fluids.[22–24] Despite the inferior RNA cleavage kinetics displayed by Zn^{2+}-neocuproine PNAzymes[13] compared to their Cu^{2+}-dependent counterparts,[12,14,15] the great potential of biocompatible artificial ribonucleases warrants further research into Zn^{2+}-dependent PNAzymes.

Herein, we report on Zn^{2+}-dimethyl-dipyridophenazine (dppz) as "molecular scissors" conjugated to PNA, creating novel biocompatible Zn^{2+} PNAzymes. Initially, 3,6-dimethyl-dipyrido[3,2-*a*:2′,3′-*c*]phenazine)-11-carboxylic acid was synthesised and conjugated to a PNA designed to target a leukaemia-related bcr/abl mRNA model (RNA 1, Fig. 1a) (see ESI,† S1 and S2). The placement of "molecular scissors" in a central part of the RNA/PNAzyme complex ensures that the cleavage of the RNA leaves the complex destabilised and prone to dissociation, which in turn facilitates turnover of the substrate.[25] However, the formation of a double strand creates a barrier for RNA cleavage since RNA is cleaved significantly more slowly in a double strand than a single strand.[26] This is likely due to an energy penalty from disruption of hydrogen bonding required to achieve the conformational change needed for the intramolecular attack of the 2′-OH group on the vicinal phosphodiester. Therefore, partial complementarity is exploited to force the formation of a

[a] *Department of Biosciences and Nutrition, Karolinska Institutet, Neo, 141 83 Huddinge, Sweden. E-mail: Roger.Stromberg@ki.se*
[b] *Oligonucleotide Discovery, Discovery Sciences, BioPharmaceuticals R&D, AstraZeneca, Gothenburg, Sweden*
[c] *DMPK, Research and Early Development, Cardiovascular, Renal and Metabolism, BioPharmaceuticals R&D, AstraZeneca, Gothenburg, Sweden*

† Electronic supplementary information (ESI) available: HPLC chromatograms and MS data for the presented RNA cleavage as well as control experiments, Zn^{2+} dependence study and a full description of the experimental work available. See DOI: 10.1039/d1cc04383h

‡ Current address: TNO Delft, Leeghwaterstraat 44. NL-2628 CA Delft, Netherlands.

§ Current address: Carrer can Vinyalets, 11, 08130 Santa Perpètua de Mogoda, Spain.

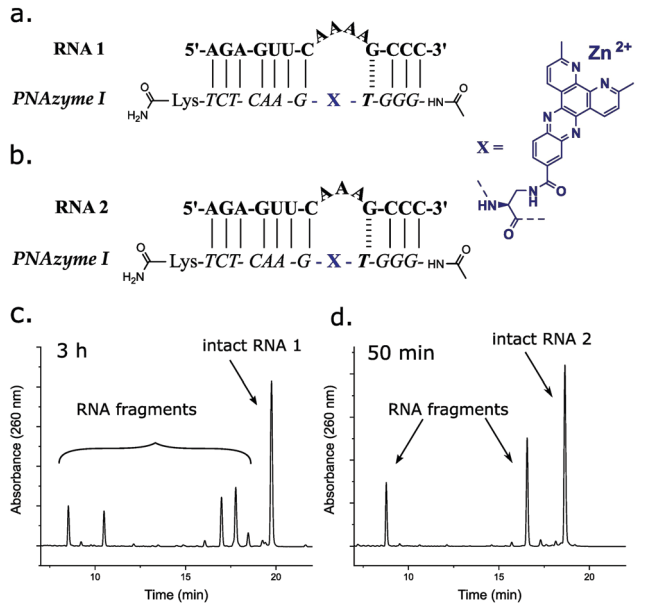

Fig. 1 Schematic representations of PNAzyme I complexes with (a) RNA 1 and (b) RNA 2 where single stranded RNA bulges of 4 or 3 adenosine nucleotides are formed. Ion-exchange HPLC chromatograms showing the extent of cleavage of (c) RNA 1 (51 ± 2% in 3 h) and (d) RNA 2 (44 ± 2% in 50 min) after incubation at 37 °C, pH 7 and 4 μM RNA/PNAzyme concentration in the presence of 100 μM Zn^{2+}.

more cleavage-prone single-stranded bulge region in the RNA, adjacent to the "molecular scissors" moiety.

In the RNA 1/PNAzyme I complex, a 4-nucleotide AAAA bulge is formed in the RNA (Fig. 1a). Cleavage of RNA 1 was observed in the presence of equimolar Zn^{2+} PNAzyme I with a half-life of 3 h at pH 7 at 37 °C (Fig. 1c). A significantly higher cleavage rate was observed for RNA 2, where a 3-nucleotide AAA bulge (Fig. 1b) was cleaved with a 1 h half-life at a single site (Fig. 1d). In prior reports, these RNAs were cleaved at multiple sites by the Zn^{2+}-neocuproine PNAzyme with *ca.* 12 and 24 h half-lives, while 7–8 h cleavage half-lives were achieved for the most rapidly cleaved RNA target sequences.[13] As such, the Zn^{2+} dimethyl-dppz PNAzyme shows unprecedented efficiency and specificity for Zn^{2+}-dependent artificial ribonucleases.

The RNA/PNAzyme complex that leads to this efficient site-specific RNA cleavage is likely to be governed by potential interactions that the novel "molecular scissors" can have with the RNA nucleobases. Aromatic heterocycles containing large rigid hydrophobic surfaces such as dppz are known intercalators, and thus prone to interact by stacking on to the heterocyclic bases in nucleic acids.[27] In fact, intercalative binding between dppz and nucleic acids has been utilised in various applications.[28–31] Increased rigidity and interactions with the dimethyl-dppz chelating moiety can result in pre-organisation of the RNA bulge, potentially making the bulge more susceptible to cleavage and possibly also helping to optimise the position of the metal ion to allow for more efficient catalysis. The presence of interactions involving dimethyl-dppz was confirmed by thermal melting analysis, which showed an increase in the RNA/PNA melting temperature from 52 to 56 °C in the presence of the covalently linked dimethyl-dppz moiety (see ESI,† S1). A prominent change was also observed in the CD spectrum, where the presence of dimethyl-dppz was clearly shown to affect the interaction in the complex (see ESI,† S1).

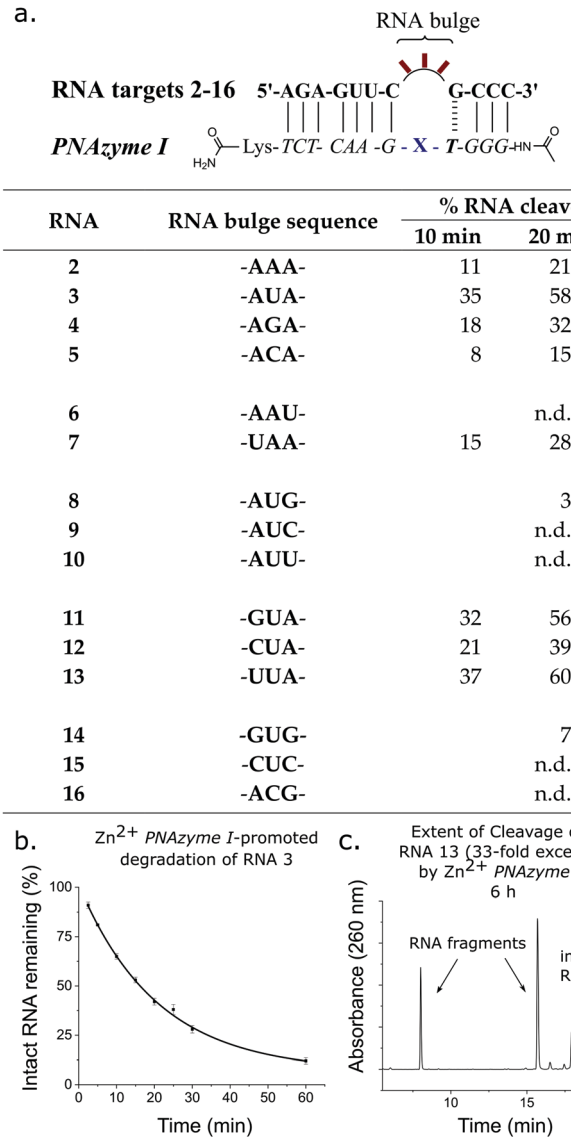

RNA	RNA bulge sequence	% RNA cleaved	
		10 min	20 min
2	-AAA-	11	21
3	-AUA-	35	58
4	-AGA-	18	32
5	-ACA-	8	15
6	-AAU-		n.d.
7	-UAA-	15	28
8	-AUG-		3
9	-AUC-		n.d.
10	-AUU-		n.d.
11	-GUA-	32	56
12	-CUA-	21	39
13	-UUA-	37	60
14	-GUG-		7
15	-CUC-		n.d.
16	-ACG-		n.d.

Fig. 2 (a) Schematic representation of PNAzyme I complexes with 3-nucleotide bulge-forming RNAs 2–16 and the extent of RNA cleavage observed for each bulge sequence. (b) RNA 3 degradation curve in the presence of Zn^{2+} PNAzyme I at pH 7. (c) Representative chromatogram of turnover experiments where the mean cleavage of RNA 13 in 6 experiments was 86 ± 4%.

The sequence of the RNA bulge is highly likely to influence the interactions in the vicinity of the cleavage site. The rate of RNA cleavage was indeed improved further when the AAA bulge was replaced with AUA, GUA or UUA bulges (RNA 3, 11, 13, Fig. 2a). The observed half-lives were now as low as 16 minutes, making the Zn^{2+} dimethyl-dppz PNAzyme presented herein the most efficient oligonucleotide-based artificial ribonuclease reported, showing unprecedented activity and site-specificity for Zn^{2+}-dependent systems[13] and displaying rates even higher

than the most efficient Cu^{2+} based systems.[12,14,15] The UA internucleosidic phosphate linkage was confirmed as the site of cleavage by ESI-MS analysis in the most rapidly cleaved RNA targets. The central uridine in the bulge provides the 2′-hydroxyl nucleophile for attack on the adjacent phosphodiester bond in the cleavage site, leading to the formation of the 2′,3′-cyclic phosphate in the longer fragment, while the adenosine 5′-hydroxyl is the leaving group in the shorter fragment (ESI-MS data presented in ESI,† S1). The degradation curve for the cleavage of RNA 3 by PNAzyme I is depicted in Fig. 2b and the characteristic cleavage patterns for RNAs 2–16 are shown in ESI,† S3.

The critical importance of the artificial enzyme as well as the metal cofactor was demonstrated, as the RNA remained intact even after 24 h of incubation if either the PNAzyme or Zn^{2+} ions were absent (see ESI,† S4). The PNAzyme was shown to give turnover of the RNA substrate, as 86 ± 4% of RNA 13 was cleaved in 6 h when the RNA was present in a 33-fold excess compared to the PNAzyme (Fig. 2c).

Zn^{2+}-Dependent PNAzyme I-promoted cleavage of RNA 3 displayed a pH-rate profile with a distinctive bell shape and an optimum at pH 7.4, where the estimated half-life of RNA cleavage was 10 minutes (Fig. 3a). This amounts to a 40–50-fold reduction in the cleavage half-life compared to Zn^{2+}-neocuproine PNAzymes at the same pH.[13] The bell-shaped pH-rate profile obtained for the PNAzyme-mediated RNA cleavage is indicative of acid–base catalysis, where one part is deprotonation of the 2′-OH nucleophile and the other part is protonation of the leaving 5′-oxygen. Varying the buffer concentration at the same pH did not affect the rate (see ESI,† S5) which suggests that general base catalysis is not present and that the deprotonation equilibrium of the 2′-OH, *i.e.* specific base catalysis, is responsible for the increase in rate of cleavage between pH 6.8 and 7.4.[32] A further increase in pH from 7.4 to 8.0 leads to a decrease in the rate which fits with the shifting of the equilibrium of the metal-aqua complex (that can protonate the 5′-O leaving group) towards the inactive metal–hydroxide.[32] It has been suggested that zinc aquo ions can exert general acid catalysis in this fashion while forming a six-membered ring (O–P–O–Zn^{2+}–O–H) complex that can protonate the leaving group.[33] A hypothetical mechanism involving a pre-equilibrium deprotonation followed by general acid catalysis by the metal aquo ion can be envisaged (Fig. 3b). This mechanism could be favoured, since the 5′-O leaving typically is limiting for non-catalysed cleavage, but other options can be considered: (1) deprotonation of the 2′-OH *via* coordination (direct or mediated by a water molecule) (2) coordination to water and hydroxide, the latter deprotonating 2′-OH and the former replaced by the phosphate to assert Zn^{2+} Lewis acid catalysis. Steric aspects may here become limiting, but it would fit the pH rate profile as deprotonation of the water prevents phosphate binding and eliminates catalysis.

Moreover, further factors, such as interactions of the chelate with nucleobases, positioning of the chelate *etc.* are likely to be important, but more structural information is needed to elucidate more details of the mechanism.

An important aspect of the PNAzymes is their adaptability to different target sequences, including clinically relevant therapeutic targets. PNAzymes could have diverse applications in disease therapy as well as molecular biology research, but the sensitivity to small structural changes in the RNA/PNAzyme complex increases uncertainty around whether it is possible to design a PNAzyme towards a desired target. In order to demonstrate the possibility to tailor PNAzymes for the cleavage of clinically relevant RNA sequences, we investigated a *Plasmodium falciparum* (malaria parasite) mRNA model as well as a SARS-CoV-2 genomic RNA model as targets for Zn^{2+} PNAzymes. We selected suitable targets with partial sequence similarities to our most rapidly cleaved RNA models, particularly the bulge sequence and the bulge closing base pairs. RNA 17 (Fig. 4a) is a model target from the *Plasmodium falciparum* exported protein 1 (EXP1) transcript which encodes an integral membrane protein essential for nutrient uptake.[34,35] RNA 18 (Fig. 4b) is a fragment originating from the genomic RNA of SARS-CoV-2 that encodes a viral protease (betacoronavirus papain-like protease, SCoV2-PLpro) which is essential for processing viral polyproteins required for a functional replicase complex that enables viral spread.[36] The cleavage of the *Plasmodium falciparum* mRNA fragment as well as the SARS-CoV-2 genomic RNA fragment by the corresponding PNAzymes proceeded as efficiently as the most rapidly cleaved RNA models above (Fig. 4c–e). As such, the Zn^{2+} PNAzymes are proving to be efficient and versatile agents that can be designed to cleave various RNA targets in a sequence and site-specific manner.

PNAzyme reliance on a sufficient local concentration of the metal cofactor is a requirement for efficient activity (see Zn^{2+} dependence in ESI,† S6, which is similar in the Zn^{2+} neocuproine systems[6,13]). The cellular Zn^{2+} can vary (0.2–0.3 mM on average, but most of it tightly bound),[22,24] while some disease conditions are associated with significantly elevated Zn^{2+} levels.[37,38] Malaria is a particularly interesting candidate for future PNAzyme developments, as extreme accumulation of zinc ions has been detected in malaria-infected red blood cells (1 mM average cellular Zn^{2+}), where free Zn^{2+} is required for parasitic growth.[37] We hope that these findings encourage further research into Zn^{2+} PNAzymes as biocompatible artificial ribonucleases that can be used as tools for molecular biology research or as candidates for therapeutic intervention.

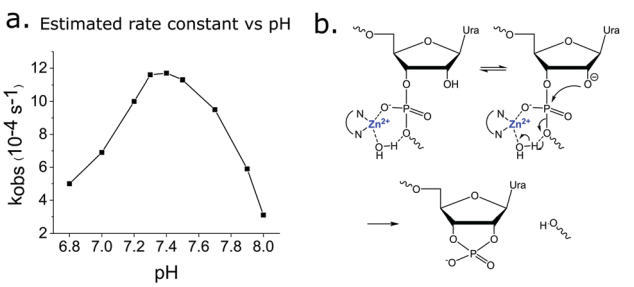

Fig. 3 (a) pH-Rate profile for RNA 3 cleavage by Zn^{2+} PNAzyme I. (b) Hypothetical mechanism for the acid–base catalysis of cleavage of RNA by Zn^{2+} dimethyl-dppz-PNAzymes.

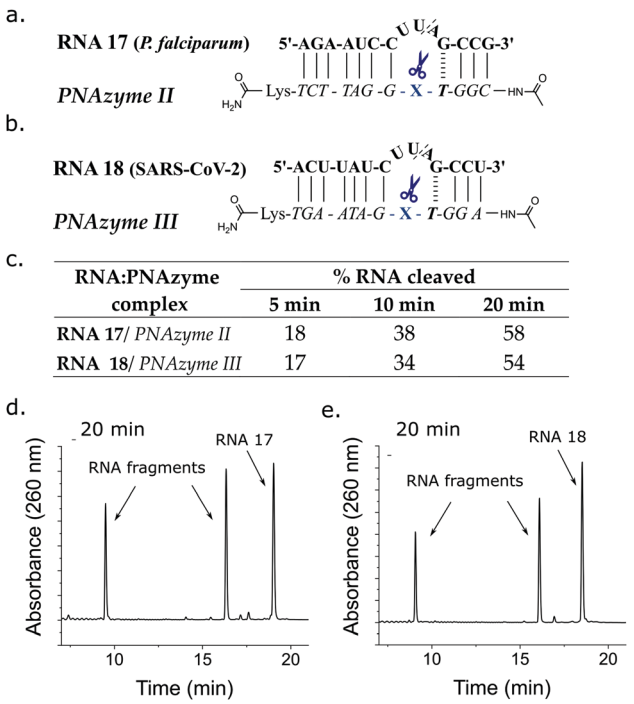

RNA:PNAzyme complex	% RNA cleaved		
	5 min	10 min	20 min
RNA 17/ *PNAzyme II*	18	38	58
RNA 18/ *PNAzyme III*	17	34	54

Fig. 4 Schematic representations of PNAzymes II and III in complex with their respective clinically relevant RNA targets (a) a *Plasmodium falciparum* (malaria parasite) mRNA model target RNA 17 and (b) a SARS-CoV-2 genomic RNA model target RNA 18. (c) The extent of cleavage of RNA 17 and 18 by PNAzymes II and III, respectively. Ion-exchange HPLC chromatograms showing the extent of cleavage of (d) RNA 17 (58 ± 2%) and (e) RNA 18 (54 ± 2%) after 20 minutes of incubation at 37 °C, pH 7 and 4 μM RNA/PNAzyme concentration in the presence of 100 μM Zn^{2+}.

Conceptualisation – M. M. and R. S. Formal analysis – O. L. and R. S. Funding acquisition – R. S. Investigation – O. L with contributions from P. B., R. Stulz, P. S., O. B., M. M. Methodology – O. L., P. S., M. M., R. S. Project administration – O. L., M. M., R. S. Resources – S. A. and R. S. Supervision – S. A., M. M., R. S. Visualisation – O. L. Writing – original draft – O. L. Writing – review and editing – O. L. and R. S. with contributions from all.

The authors would like to extend their gratitude to the Separation Science Laboratory at AstraZeneca Gothenburg for experimental assistance and advice on RNA purification. Eva-Lotta Käsper and Johanna Luige are acknowledged for helpful discussions and advice. This project has received funding from the European Union's Horizon 2020 research and innovation programme under the Marie Skłodowska-Curie grant agreement no. 721613. This material reflects only the authors' views and the Union is not liable for any use that may be made of the information contained therein.

Conflicts of interest

There are no conflicts to declare.

References

1 S. T. Crooke, B. F. Baker, R. M. Crooke and X. Liang, *Nat. Rev. Drug Discovery*, 2021, **20**, 427–453.
2 Y. Aoki and M. J. A. Wood, *J. Neuromuscul. Dis.*, 2021, 1–16.
3 A. Khvorova and J. K. Watts, *Nat. Biotechnol.*, 2017, **35**, 238–248.
4 T. C. Roberts, R. Langer and M. J. A. Wood, *Nat. Rev. Drug Discovery*, 2020, **19**, 673–694.
5 D. Grimm, K. L. Streetz, C. L. Jopling, T. A. Storm, K. Pandey, C. R. Davis, P. Marion, F. Salazar and M. A. Kay, *Nature*, 2006, **441**, 537–541.
6 H. Åström, N. H. Williams and R. Strömberg, *Org. Biomol. Chem.*, 2003, **1**, 1461–1465.
7 H. Åström and R. Strömberg, *Org. Biomol. Chem.*, 2004, **2**, 1901–1907.
8 M. Murtola and R. Strömberg, *ARKIVOC*, 2009, 84–94.
9 A. Kuzuya and M. Komiyama, *Curr. Org. Chem.*, 2007, **11**, 1450–1459.
10 T. Niittymäki and H. Lönnberg, *Org. Biomol. Chem.*, 2006, **4**, 15–25.
11 A. Ghidini, M. Murtola and R. Strömberg, *DNA in Supramolecular Chemistry and Nanotechnology*, John Wiley and Sons, Ltd, Hoboken, NJ, USA, 1st edn, 2015, pp. 158–171.
12 O. Luige, M. Murtola, A. Ghidini and R. Strömberg, *Molecules*, 2019, **24**, 672.
13 M. Murtola, A. Ghidini, P. Virta and R. Strömberg, *Molecules*, 2017, **22**, 1856.
14 A. Ghidini, M. Murtola and R. Strömberg, *Org. Biomol. Chem.*, 2016, **14**, 2768–2773.
15 M. Murtola, M. Wenska and R. Strömberg, *J. Am. Chem. Soc.*, 2010, **132**, 8984–8990.
16 F. Zellmann and M. W. Göbel, *Molecules*, 2020, **25**, 1842.
17 F. Zellmann, L. Thomas, U. Scheffer, R. K. Hartmann and M. W. Göbel, *Molecules*, 2019, **24**, 807.
18 Y. Staroseletz, B. Amirloo, A. Williams, A. Lomzov, K. K. Burusco, D. J. Clarke, T. Brown, M. A. Zenkova and E. V. Bichenkova, *Nucleic Acids Res.*, 2020, **48**, 10662–10679.
19 M. Gebrezgiabher, W. A. Zalloum, D. J. Clarke, S. M. Miles, A. A. Fedorova, M. A. Zenkova and E. V. Bichenkova, *J. Biomol. Struct. Dyn.*, 2020, 1–20.
20 O. Patutina, D. Chiglintseva, E. Bichenkova, S. Gaponova, N. Mironova, V. Vlassov and M. Zenkova, *Molecules*, 2020, **25**, 2459.
21 Z. N. Baker, P. A. Cobine and S. C. Leary, *Metallomics*, 2017, **9**, 1501–1512.
22 D. Beyersmann, *Materwiss. Werksttech.*, 2002, **33**, 764–769.
23 R. B. Franklin, J. Ma, J. Zou, Z. Guan, B. I. Kukoyi, P. Feng and L. C. Costello, *J. Inorg. Biochem.*, 2003, **96**, 435–442.
24 I. Sekler, S. L. Sensi, M. Hershfinkel and W. F. Silverman, *Mol. Med.*, 2007, **13**, 337–343.
25 D. Hüsken, G. Goodall, M. J. J. Blommers, W. Jahnke, J. Hall, R. Häner and H. E. Moser, *Biochemistry*, 1996, **35**, 16591–16600.
26 U. Kaukinen, L. Bielecki, S. Mikkola, R. W. Adamiak and H. Lönnberg, *J. Chem. Soc., Perkin Trans. 2*, 2001, 1024–1031.
27 A. Mukherjee and W. D. Sasikala, *Advances in Protein Chemistry and Structural Biology*, Academic Press, Elsevier Inc., 2013, vol. 92, pp. 1–62.
28 G. Li, L. Sun, L. Ji and H. Chao, *Dalton Trans.*, 2016, **45**, 13261–13276.
29 A. E. Friedman, J. K. Barton, J. C. Chambron, J. P. Sauvage, N. J. Turro and J. K. Barton, *J. Am. Chem. Soc.*, 1990, **112**, 4960–4962.
30 A. J. McConnell, H. Song and J. K. Barton, *Inorg. Chem.*, 2013, **52**, 10131–10136.
31 S. T. Li, Z. Y. Ma, X. Liu, J. L. Tian and S. P. Yan, *Appl. Organomet. Chem.*, 2017, **31**, 1–14.
32 J. R. Morrow and O. Iranzo, *Curr. Opin. Chem. Biol.*, 2004, **8**, 192–200.
33 S. Mikkola, E. Stenman, K. Nurmi, E. Yousefi-Salakdeh, R. Strömberg and H. Lönnberg, *J. Chem. Soc., Perkin Trans. 2*, 1999, 1619–1626.
34 K. Günther, M. Tümmler, H. H. Arnold, R. Ridley, M. Goman, J. G. Scaife and K. Lingelbach, *Mol. Biochem. Parasitol.*, 1991, **46**, 149–157.
35 P. Mesén-Ramírez, B. Bergmann, T. T. Tran, M. Garten, J. Stäcker, I. Naranjo-Prado, K. Höhn, J. Zimmerberg and T. Spielmann, *PLoS Biol.*, 2019, **17**, 1–33.
36 D. Shin, R. Mukherjee, D. Grewe, D. Bojkova, K. Baek, A. Bhattacharya, L. Schulz, M. Widera, A. R. Mehdipour, G. Tascher, P. P. Geurink, A. Wilhelm, G. J. van der Heden van Noort, H. Ovaa, S. Müller, K. P. Knobeloch, K. Rajalingam, B. A. Schulman, J. Cinatl, G. Hummer, S. Ciesek and I. Dikic, *Nature*, 2020, **587**, 657–662.
37 R. G. Marvin, J. L. Wolford, M. J. Kidd, S. Murphy, J. Ward, E. L. Que, M. L. Mayer, J. E. Penner-Hahn, K. Haldar and T. V. O'Halloran, *Chem. Biol.*, 2012, **19**, 731–741.
38 T. J. A. Craddock, J. A. Tuszynski, D. Chopra, N. Casey, L. E. Goldstein, S. R. Hameroff and R. E. Tanzi, *PLoS One*, 2012, **7**, e33552.

